stay close to the simulated one, although it has some ripples. As for the measured loss constant, it is obviously higher than the simulated one, which indicates that the actual sample is more lossy. Possible reasons may lie in that the loss characteristics of the materials tend to be worse at higher frequencies and the bond between the LTCC and PCB board might not be perfect. Nevertheless, 1.4 Np/m or 12.1 dB/m at 35 GHz is still an excellent loss performance.

4. CONCLUSION

Through the EDC method, a DIIG is designed .Calculated results are compared with those from the rigorous FEM method, which shows good agreements. DIIGs comprising LTCC dielectric rods on RT Duroid substrate have been fabricated. Good agreement between theory and measurement has been demonstrated for the phase constant and the attenuation constant of 12.1 dB/m at 35 GHz is an excellent loss performance. Further application of this analysis, and fabrication using other materials, can be expected to yield excellent results at higher frequencies, potentially even in the terahertz region.

ACKNOWLEDGMENT

Part of this work was sponsored by the Engineering and Physical Sciences Research Council (EPSRC) in the project "3D Microwave and Millimetre-Wave System-on-Substrate using Sacrificial Layers for Printed MEMS components" in collaboration with Loughborough University and Imperial College London.

REFERENCES

1. S.K. Koul (Ed.), Millimeter wave and optical dielectric integrated guides and circuits, 1st ed., Wiley-Interscience, New York, 1997.
2. D.D. King, Dielectric image lines, J Appl Phys 23 (1952), 699–700.
3. R. Knox, Dielectric waveguide microwave integrated circuits—an overview, IEEE Trans Microwave Theory Tech 24 (1976), 806–814.
4. L. Jin, R. Lee, and I. Robertson, Modelling of a double-sided dielectric resonator antenna array fed from dielectric insular image guide, In: Antennas and Propagation Conference (LAPC), Loughborough, 2012, pp. 1–4.
5. E.A.J. Marcatili, Dielectric rectangular waveguide and directional coupler for integrated optics, Bell Syst Tech J 48 (1969), 2071–2102.
6. R.M. Knox and P.P. Toulios, Integrated circuits for the millimeter through optical frequency range, In: Proceedings of the Symposium on Submillimeter Waves, New York, 1970, pp. 497–516.
7. S. Peng and A. Oliner, Guidance and leakage properties of a class of open dielectric waveguides: Part I-mathematical formulations, IEEE Trans Microwave Theory Tech 29 (1981), 843–855.
8. R. Mittra, Y.-L. Hou, and V. Jamnejad, Analysis of open dielectric waveguides using mode-matching technique and variational methods, IEEE Trans Microwave Theory Tech 28 (1980), 36–43.
9. J.E. Goell, A circular-harmonic computer analysis of rectangular dielectric waveguides, Bell Syst Tech J 48 (1969), 2133–2160.
10. K. Ogusu, Numerical analysis of the rectangular dielectric waveguide and its modifications, IEEE Trans Microwave Theory Tech 25 (1977), 874–885.
11. M. Ikeuchi, H. Sawami, and H. Niki, Analysis of open-type dielectric waveguides by the finite-element iterative method, IEEE Trans Microwave Theory Tech 29 (1981), 234–240.
12. F. Xu and K. Wu, Guided-wave and leakage characteristics of substrate integrated waveguide, IEEE Trans Microwave Theory Tech 53 (2005), 66–73.

A COMPACT ANTENNA WITH FREQUENCY AND PATTERN RECONFIGURABLE CHARACTERISTICS

Yong Pan,[1,2] Yongta Ma,[2] Jiang Xiong,[1] Ziye Hou,[1] and Yue Zeng[1]

[1] School of Computer Science and Engineering, Chongqing Three Gorges University, Chongqing 404100, China

[2] School of Electronic Information Engineering, Tianjin University, Tianjin 300072, China; Corresponding author: zhurongji_211@163.com

Received 30 March 2015

ABSTRACT: *This article proposes a compact printed frequency and pattern reconfigurable antenna. The antenna has a low profile, low cost, and small size of 58.0 × 40.0 × 1.2 mm^3, and mainly consists of dual symmetrical radiators, two rectangle parasitic elements and one inverted T-shape ground plane which may acts as a reflector. By loading the parasitic elements and selecting different radiators to connect to the feed, the proposed antenna can switch among three operating frequencies (2.01–2.26 GHz, 2.28–2.52 GHz, and 3.73–4.02 GHz) and select patterns between two kinds of radiating patterns with main lobe directions of φ = 90° and φ = 270° in the xoy plane. Comparing the expected results with measured results, a good agreement is obtained.*

 Microwave Opt Technol Lett 55:2467–2471, 2015; View this article online at wileyonlinelibrary.com. DOI 10.1002/mop.29371

Key words: *directive antenna; reconfigurable architecture; symmetrical structure*

1. INTRODUCTION

MORE and more attention has been drawn on reconfigurable antennas since the plan of "Reconfigurable Aperture Program" was drawn up by the U.S. Defense Advanced Research Projects Agency (DARPA) in 1999 [1], owing to they can dynamically tune their electrical characteristics, such as operating frequencies, radiation patterns, or polarization modes. Generally, they are divided as frequency, pattern and polarization reconfigurable antennas according to their functions [2]. The frequency reconfigurable antenna intends to alter its operating frequencies while keeping the radiation patterns and polarization unchanged. Similarly, the pattern and polarization reconfigurable antennas are to change the radiation patterns and polarization modes merely, respectively. The antennas with reconfigurable characteristics are very helpful to reduce system size, suppress noise, avoid electronic jamming, save energy and improve security [3].

One way to obtain the reconfigurable characteristics is to change the surface current distributions by modifying the corresponding local structure. Some electronic components, such as PIN diodes, varactor diodes, FET and MEMS switches, were used to achieve the reconfigurable traits by changing the effective radiated electrical length, selecting the radiating elements or changing feeding position electronically [4–8].

Another method is to make full use of the array antennas [9–11]. In [10,11], array antennas which were composed of a number of metallic patches interconnected by MEMS actuators have been proposed. But those antennas may be too large, too complex and too costly to meet the needs of common engineering applications [12].

In this article, a novel frequency and pattern reconfigurable antenna is presented. By loading parasitic elements, the antenna is capable of switching among three operating bands: 2.01–2.26 GHz, 2.28–2.52 GHz, and 3.73–4.02 GHz, which can be used

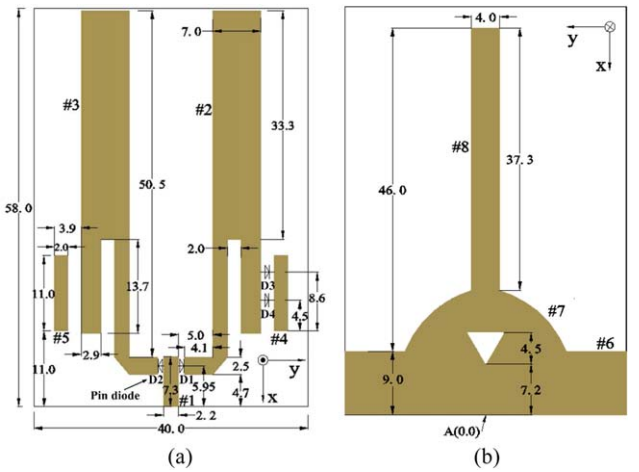

Figure 1 Configuration and geometry of the proposed antenna. (a) Top view and (b) bottom view. [Color figure can be viewed in the online issue, which is available at wileyonlinelibrary.com]

in systems of UMTS (1920–2170 MHz), WCDMA (1920–2170 MHz), Wibro (2300–2390 MHz), Bluetooth (2400–2484 MHz), Zigbee (2400–2485 MHz), satellite C band (3.7–4.2 GHz), and WLAN (2400–2480 MHz) [13,14]. With changing the connections between the feed and radiators, the beams can be steered in the direction of $\varphi = 90^\circ$ and $\varphi = 270^\circ$ in *xoy* plane ($\theta = 90^\circ$), respectively.

The article is organized in the following sections. Section 2 describes the design of the reconfigurable antenna. Section 3 illustrates the operation mechanism and analyzes the simulated and measured results of proposed antenna briefly. Section 4 summarizes and concludes this study.

2. ANTENNA STRUCTURE AND DESIGN

The optimized configuration and geometry of the proposed antenna is shown in Figure 1. The antenna, fabricated on a FR-4 epoxy substrate with the thickness of 1.2 mm and relative dielectric constant of 4.4, consists of one rectangle microstrip transmission line (#1), two symmetrical radiators (#2, #3), two rectangle parasitic elements (#4, #5) and one inverted T-shape ground plane (#6, #7, #8). On the top of substrate, the radiators are fed by microstrip transmission line which is terminated with a subminiature A (SMA) connector.

The characteristic impedance Z_d of microstrip transmission line #1 has a great influence on the state of impedance matching at desired resonant frequencies. So, one significant step of the design is to adjust Z_d to 50 Ω approximately. The value of Z_d is determined approximately by the empirical formula as follows,

$$Z_d = \frac{1}{\sqrt{\varepsilon_{\text{eff}}}} \frac{120\pi}{\frac{W}{h} + 2.42 - 0.44\frac{h}{W} + \left(1 - \frac{h}{W}\right)^6} \Omega \left(\frac{W}{h} \geq 1\right) \quad (1)$$

TABLE 1 The Operative Modes of Proposed Reconfigurable Antenna

Mode	Switches ON	Frequency (GHz)	Main lobe direction $\theta = 90^\circ$
1	D1	2.28–2.52	$\varphi = 90^\circ$
2	D2	2.28–2.52	$\varphi = 270^\circ$
3	D1, D3	2.01–2.26	$\varphi = 90^\circ$
4	D1, D4	3.73–4.02	$\varphi = 90^\circ$

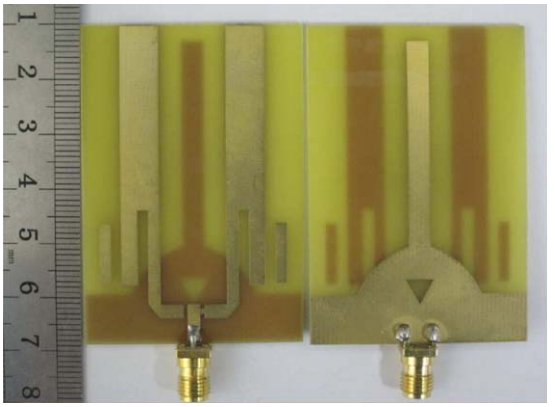

Figure 2 Photograph of Mode 1 of the proposed antenna. [Color figure can be viewed in the online issue, which is available at wileyonlinelibrary.com]

$$\varepsilon_{\text{eff}} = \frac{\varepsilon_r + 1}{2} + \frac{\varepsilon_r - 1}{2}\left(1 + \frac{10h}{W}\right)^{-1/2} \quad (2)$$

Where, W in millimeters is the width of microstrip feed (#1), h in millimeters presents the thickness of substrate, ε_r and ε_{eff} are the relative and effective dielectric constant, respectively.

Generally, the microstrip antenna operates in its resonant states. In this article, the length of radiators is selected to be three-quarter effective operating wavelength. The relationship between the total length of radiators and resonant frequency can be summarized as following formula [15],

$$L_{\text{rad}} = 0.75\lambda_{\text{eff}} = \frac{0.75c}{f_{\text{res}}\sqrt{\varepsilon_{\text{eff}}}}\text{mm} \quad (3)$$

Where, L_{rad} in millimeters is the length of radiators (2, #3), λ_{eff} is effective wavelength, f_{res} in GHz is resonant frequency and c is the speed of the light in free space.

It is mentioned that, the part #7 of ground plane is a portion of an ellipse and acts as an impedance transformer between part #6 and #8. If we set the starting point coordinate of ground plane in *x*-*y* plane ($\theta = 90^\circ$) as A (0, 0), as shown in Figure 1 (b), the ellipse will have the central point coordinate (4.1, 0), major and minor axis of 22 mm and 14.3 mm, respectively. The length of part #8 is shorter than that of radiator and it woks as a reflector.

By controlling the states of different switches, the proposed antenna can switch among reconfigurable radiating patterns and frequencies, as shown in Table 1. The photograph of Mode 1 of proposed antenna is shown in Figure 2.

3. RESULTS AND DISCUSSIONS

In this article, the presented antenna was simulated by the electromagnetic software Ansoft HFSS 13.0 and measured by the network analyzer Agilent E5071B ENA (300 KHz–8.5 GHz). To be simple and validate the reconfigurable concept, the states of the switches were replaced by the copper strip or air gap.

3.1. Input Impedance Matching and Resonant States

It is known that the input impedance matching at desired frequencies is essential to the resonant antenna. Generally, the antenna is fed by coaxial cable with characteristic impedance of 50 Ω. So, one of the most important steps of the design process

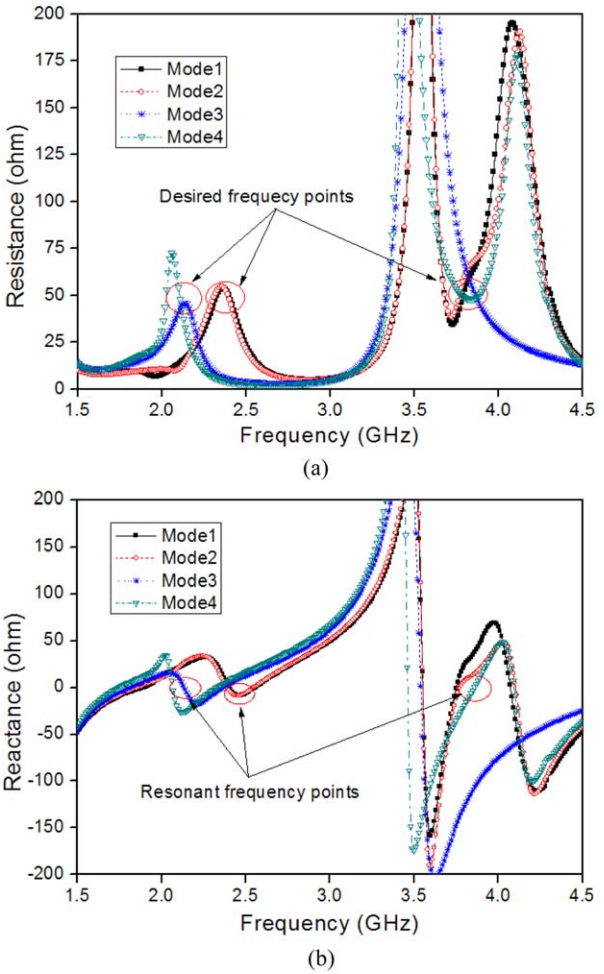

Figure 3 The simulated input resistance and reactance of proposed antenna. (a) Resistance and (b) reactance. [Color figure can be viewed in the online issue, which is available at wileyonlinelibrary.com]

is to adjust the resistance and reactance at desired frequencies to be 50 Ω and 0 Ω, respectively. As shown in Figure 3, the simulated results of resistance and reactance are given. It is evident that the antenna resistance and reactance are much closed to 50 Ω and 0 Ω at desired frequencies, respectively. That is to say,

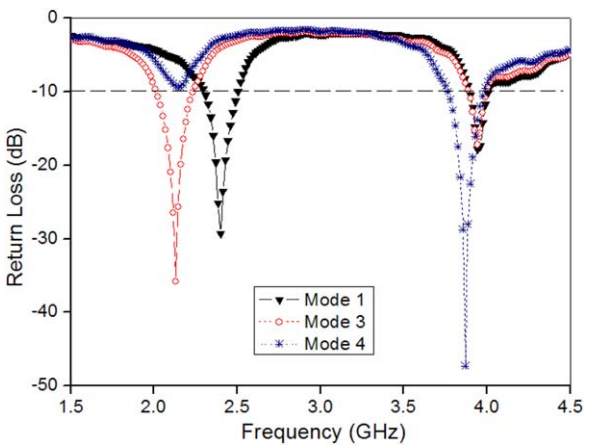

Figure 4 The measured return losses of Mode 1, Mode 3, and Mode 4. [Color figure can be viewed in the online issue, which is available at wileyonlinelibrary.com]

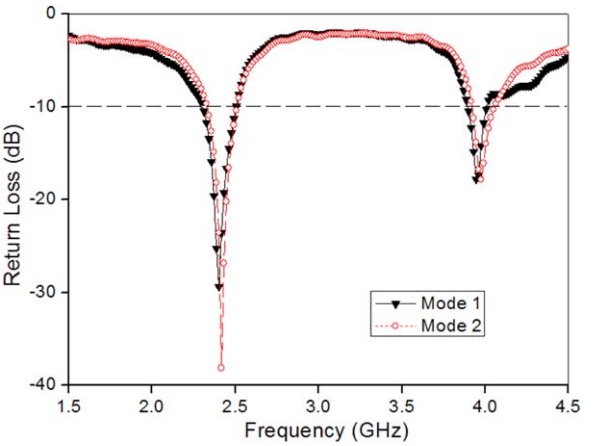

Figure 5 The measured return losses of Mode 1 and Mode 2. [Color figure can be viewed in the online issue, which is available at wileyonlinelibrary.com]

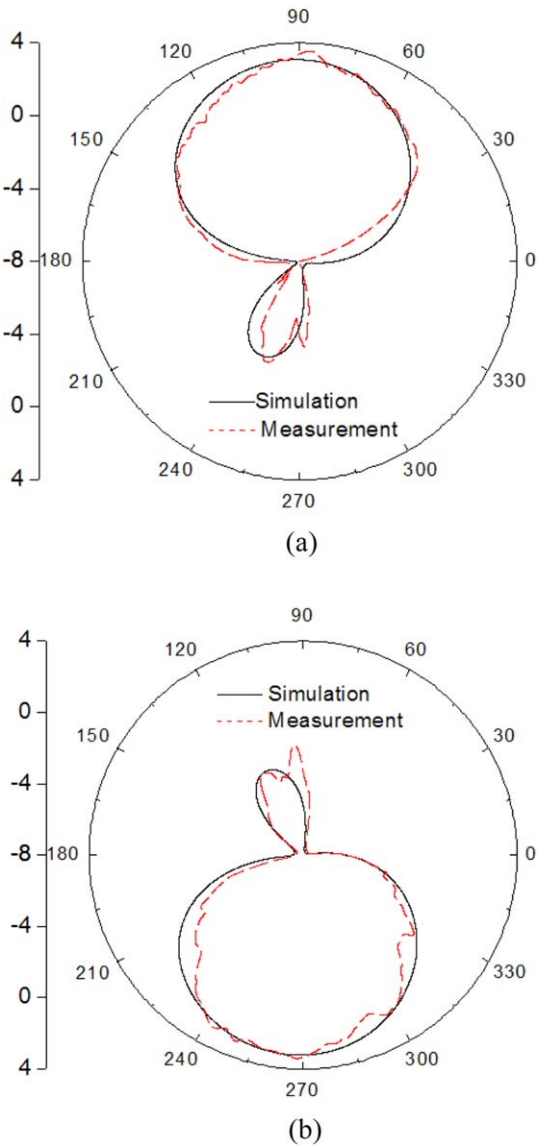

Figure 6 The simulated and measured patterns in xoy plane at 2.4 GHz. (a) Mode 1 and (b) Mode 2. [Color figure can be viewed in the online issue, which is available at wileyonlinelibrary.com]

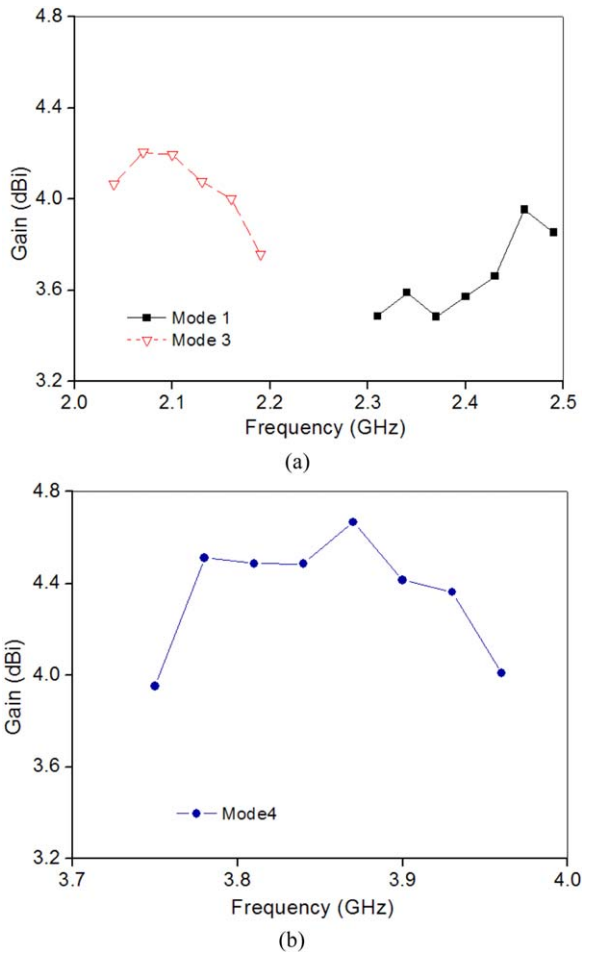

Figure 7 Measured gains of different modes of proposed antenna. (a) Mode 1 and Mode 3 and (b) Mode 4. [Color figure can be viewed in the online issue, which is available at wileyonlinelibrary.com]

the proposed antenna is in impedance matching and resonant states at those frequencies approximately.

3.2. Frequency Reconfigurable Characteristics

By loading corresponding parasitic elements, the effective electrical length and surface current distributions of presented antenna will be changed, and then reconfigurable frequencies can be achieved. In this article, as seen in Figure 4, the proposed antenna can switch among three frequency bands of 2.01–2.26 GHz, 2.28–2.52 GHz, and 3.73–4.02 GHz.

3.3. Pattern Reconfigurable Characteristics

Figure 5 gives the curves of the measured return losses of Mode 1 and Mode 2. From the figure, the operating band with -10 dB return loss, covering the bandwidth from 2.28 GHz to 2.52 GHz, is obtained.

The simulated and measured radiating patterns in *xoy* plane ($\theta = 90°$) are presented in Figure 6. Between the measured and simulated results, a good agreement can be observed and the radiating characteristics are very stable. The Mode 1 and Mode 2 of proposed antenna have similar main lobe shapes and obviously single radiating characteristics with the main lobe direction of $\varphi = 90°$ and $\varphi = 270°$, respectively. Meanwhile, the cross-polarization radiation patterns are relatively small (not more than -16.8 dB).

3.4. Antenna Gain

Figure 7 shows the measured gains of Mode 1, Mode 3, and Mode 4. The gains of three modes are relatively high and up to 3.4–4.8 dBi. It is also concluded that, the Mode 3 and Mode 4 have higher gains than the Mode 1, owing to loading parasitic elements increase the radiating area.

4. CONCLUSION

The article introduces a novel planar antenna with frequency and radiating pattern reconfigurable characteristics. By loading the parasitic elements or not, reconfigurable frequency bands of 2.01–2.26 GHz, 2.28–2.52 GHz, and 3.73–4.02 GHz, which can be applied in the systems of UMTS, WCDMA, Wibro, Bluetooth, Zigbee, satellite C band, and WLAN, are achieved. Meanwhile, adjusting the connections between the feed and radiators, the antenna can change the main lobe direction in xoy plane. Thus, the proposed reconfigurable antenna is a good candidate in the multi-band, searching, tracking and positioning systems.

ACKNOWLEDGMENTS

This work was supported by the National Natural Science Foundation of China (61401301) and the Research Project of Chongqing Education Committee of China (KJ1401029) and the Research Foundation of Chongqing Three Gorges University of China(14RC10).

REFERENCES

1. J.K. Smith, Reconfigurable Aperture Program (RECAP), In: USA: Defense Advanced Research Projects Agency (DARPA), Arlington, VA, 1999.
2. M.-I. Lai, T.-Y. Wu, J.-C. Hsieh, C.-H. Wang, and S.-K. Jeng, Design of reconfigurable antennas based on an L-shaped slot and PIN diodes for compact wireless devices, IET Microwave Antennas Propag 3 (2009), 47–54.
3. J. Ouyang, F. Yang, and S. Yang, A novel radiation pattern reconfigurable microstrip antenna for wide-angle scanning application in phased antenna array, Microwave Opt Technol Lett 50 (2008), 1359–1340.
4. D. Peroulis, K. Sarabandi, and L.P.B. Katehi, Design of reconfigurable slot antennas, IEEE Trans Antennas Propag 53 (2005), 645–654.
5. P.-Y. Qin, A.R. Weily, Y.J. Guo, and C.-H. Liang, Polarization reconfigurable U-slot patch antenna, IEEE Trans Antennas Propag 58 (2010), 3383–3388.
6. M.K. Fries, M. Grani, and R. Vahldieck, A reconfigurable slot antenna with switchable polarization, IEEE Microwave Wireless Compon Lett 13 (2003), 490–492.
7. H.F. Abutarboush, R. Nilavalan, S.W. Cheung, K.M. Nasr, T. Peter, D. Budimir, and H. Al-Raweshidy, A reconfigurable wideband and multiband antenna using dual-patch elements for compact wireless devices, IEEE Trans Antennas Propag 60 (2012), 36–43.
8. F. Ghanem, P.S. Hall, and J.R. Kelly, Two port frequency reconfigurable antenna for cognitive radios, Electron Lett 45 (2009), 534–536.
9. Y. Cai and Z. Du, A novel pattern reconfigurable antenna array for diversity systems, IEEE Antennas Wireless Propag Lett 8 (2009), 1227–1230.
10. B.A. Cetiner, H. Jafarkhani, J.-Y. Qian, H.J. Yoo, A. Grau, and F. De Flaviis, Multifunctional reconfigurable MEMS integrated antennas for adaptive MIMO systems, IEEE Commun Mag 42 (2004), 62–70.
11. L.N. Pringle, P.H. Harms, S.P. Blalock, G.N. Kiesel, E.J. Kuster, P.G. Friederich, R.J. Prado, J.M. Morris, and G.S. Smith, A reconfigurable aperture antenna based on switched links between electrically small metallic patches, IEEE Trans Antenna Propag 52 (2004), 1434–1445.
12. S. Zhang, G.H. Huff, J. Feng, and J.T. Bernhard, A pattern reconfigurable microstrip parasitic array, IEEE Trans Antenna Propag 52 (2004), 2773–2776.
13. R.A. Bhatti, Y.-T. Im, and S.-O. Park, Compact PIFA for mobile terminals supporting multiple cellular and non-cellular standards, IEEE Trans Antennas Propag 57 (2009), 2534–2540.

14. Z. Chunna, Y. Songnan, S. El-Ghazaly, A.E. Fathy, and V.K. Nair, A low-profile branched monopole laptop reconfigurable multiband antenna for wireless applications, IEEE Trans Antenna Propag 8 (2009), 216–219.
15. B. Chen, A.-G. Wang, and G.-H. Zhao, Design of a novel ultra wideband antenna with dual band-notched characteristic, Microwave Opt Technol Lett 54 (2012), 2401–2405.

MINIATURE LOW SAR PRINTED MONOPOLE ANTENNA FOR MOBILE PHONE

M. I. Hossain,[1] M. R. I. Faruque,[1] and M. T. Islam[2]
[1] Centre of Space Science, Universiti Kebangsaan Malaysia; Corresponding author: ipk_eee@yahoo.com
[2] Department of Electrical Electronic and Systems Engineering, Universiti Kebangsaan Malaysia

Received 3 April 2015

ABSTRACT: *A multiband compact printed monopole antenna is proposed for mobile phone. In this configuration, the antenna comprises a slotted rectangular-shaped radiator, microstrip-fed line, and a slotted ground plane on FR-4 substrate. The total antenna dimensions with ground plane are 78 × 40 × 0.8 mm³. The measured results show that the proposed antenna has an impedance bandwidth 358.4 MHz (0.60–0.95 GHz, lower band), and 1 GHz (1.7–2.7 GHz, upper band), which can cover GSM 900 MHz, DCS 1800 MHz, PCS 1900 MHz, GSM 1900 MHz, UMTS 2100 MHz, Bluetooth 2400 MHz, WLAN II.b (2400 MHz), and LTE (2300–2400 MHz) bands. The proposed antenna shows very good radiation efficiencies and gain values and near omnidirectional radiation patterns at those frequency bands. Moreover, the proposed antenna produces lower specific absorption rate values in the human head than that of a dipole antenna, helical antenna, and planar inverted-F antenna.* © 2015 Wiley Periodicals, Inc. Microwave Opt Technol Lett 55:2471–2475, 2015; View this article online at wileyonlinelibrary.com. DOI 10.1002/mop.29373

Key words: *antennas; microstrip line; mobile phone; specific absorption rate*

1. INTRODUCTION

Nowadays, mobile phone antenna design is getting more concern of researchers due to the rapid advance in communication systems. Microstrip printed antennas are being popular day by day because of their intrinsic characteristics such as low profile, low cost, and easy integration possibility with other electronic and microwave components [1]. Various types of the conventional multiband internal antennas were proposed in the form of monopoles or planar inverted-F antennas (PIFAs). All those antennas operate with an additional large ground plane. But, the microstrip-fed patch antenna design technique facilitates to combine antenna radiator and ground plane in printed from on a substrate only. In [2], a mobile handset antenna combining PIFA with slotted ground plane was proposed. The antenna was placed 6 mm apart from ground plane. In [3], a multiband monopole antenna was introduced combining T-shaped bending metal plate about 6 mm above on the ground plane. In [4], a hexa-band monopole antenna was proposed for mobile phone with a large ground plane (115 × 50 mm²). A multiband antenna comprising radiator of dimensions 50 × 15 × 4 mm³ and substrate of dimensions 110 × 50 × 1 mm³ was presented as an internal handset antenna [5]. In [6], a mobile phone antenna with circular polarization was proposed with ground plane dimensions 110 × 50 × 1.6 mm³. Moreover, different types of microstrip patch antennas were also proposed in the literature for various applications. In [7], a dual band folded loop microstrip-patch antenna was designed for wireless local area network (WLAN) applications. In [8], another approach of triple-band patch antenna was proposed for PCS, WLAN, and WiMax applications. In [9], a waveguide circular-slotted patch antenna was designed and fabricated for WiFi and WiMax applications.

Recently, the biological effects of electromagnetic (EM) radiation have attracted gusto in the research community due to the fact that the EM radiation disturbs the biological system of human body [10]. To date, the World Health Organization had ruled out that the radiation from mobile phone could cause toward the public users [11]. To prevent the cell phone user from the EM exposure, safety limits are imposed usually in terms of specific absorption rate (SAR) by the authoritative

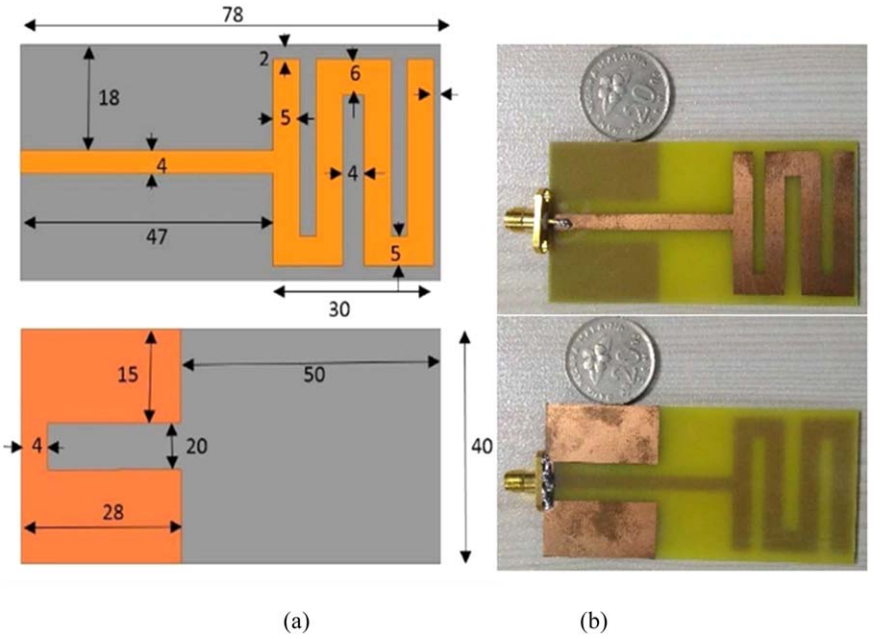

Figure 1 Proposed printed monopole antenna: (a) antenna geometry: front view (top), back view (bottom) (dimensions: millimeters), and (b) fabricated prototype of proposed antenna. [Color figure can be viewed in the online issue, which is available at wileyonlinelibrary.com]